Available online at www.sciencedirect.com
SCIENCE DIRECT®
Journal of Molecular Graphics and Modelling 23 (2005) 395–407
Journal of Molecular Graphics and Modelling
www.elsevier.com/locate/JMGM

LigScore: a novel scoring function for predicting binding affinities

André Krammer*, Paul D. Kirchhoff[1], X. Jiang, C.M. Venkatachalam, Marvin Waldman

Accelrys Inc., 10188 Telesis Court, Suite 100, San Diego, CA 92121, USA

Received 23 June 2004; received in revised form 17 October 2004; accepted 1 November 2004
Available online 25 December 2004

Abstract

We present two new empirical scoring functions, *LigScore1* and *LigScore2*, that attempt to accurately predict the binding affinity between ligand molecules and their protein receptors. The *LigScore* functions consist of three distinct terms that describe the van der Waals interaction, the polar attraction between the ligand and protein, and the desolvation penalty attributed to the binding of the polar ligand atoms to the protein and vice versa. Utilizing a regression approach on a data set of 118 protein–ligand complexes we have obtained a linear equation, *LigScore2*, using these three descriptors. *LigScore2* has good predictability with regard to experimental pK_i values yielding a correlation coefficient, r^2, of 0.75 and a standard deviation of 1.04 over the training data set, which consists of a diverse set of proteins that span more than seven protein families.
© 2004 Elsevier Inc. All rights reserved.

Keywords: LigScore; Binding affinity; Desolvation penalty

1. Introduction

We are currently at the dawn of the proteomics era. New technologies in high-throughput proteomics [1], including gene cloning, protein purification, and 3D structure determination are opening up new possibilities in structure-guided drug discovery projects. Linking these proteins with their physiological function and pharmacological significance is facilitated by genomic annotation [2–4]. However, identifying a small molecule drug candidate for a pharmacological protein target remains a daunting task that involves possibly synthesizing as well as screening up to millions of molecules against a particular target. In silico screening as a pre-selective process can therefore, in principle, help address this predicament and accelerate the development process, if it reduces the number of potential ligand molecules that need to be considered for synthesis and examined for their efficacy and mode of action in various biological assays.

In silico high-throughput screening can be roughly divided into two major steps, namely docking and scoring, that are closely intertwined with each other. The first step is often referred to as finding the right molecular ''key'' to a known receptor ''lock'' [5] with the fitting objective purely based on optimizing atomic coordinates. As an extension to the simple static ''lock'' and ''key'' view, the induced fit model [6] takes into account that the ligand and receptor possess the ability to adapt their 3D structure in such a way as to accommodate the binding to each other.

In addition to the difficulty of modeling ligand and protein flexibility, the second step in virtual screening remains in determining what constitutes a ''good fit'' between the ligand ''key'' and receptor ''lock'' that is not solely based on fitting of atomic coordinates. This issue is complicated by the fact that multiple ''fits'' of a ligand to a protein may exist and a ''fit'' might entail only a partial occupancy of the ligand to the putative protein active site. Evaluating the fit of a ligand to a protein receptor is commonly referred to as the 'scoring problem' and is closely related to the previous step of docking a ligand into the protein-binding pocket. It calls for devising a function that correctly prioritizes the docked ligand poses, and simultaneously correlates with or predicts their binding affinities.

* Corresponding author.
E-mail address: akrammer@accelrys.com (A. Krammer).
[1] Present address: Pfizer Inc., 2800 Plymouth Road, Ann Arbor, MI 48105, USA.

1093-3263/$ – see front matter © 2004 Elsevier Inc. All rights reserved.
doi:10.1016/j.jmgm.2004.11.007

While much significant progress has been made in this field (see [7,8] for reviews), no scoring function has been found that is both sufficiently accurate to reliably predict binding affinity and fast enough to address millions of ligands against a wide range of protein targets. This is due to the complex nature of molecular interactions between ligand, protein and solvent. In general, scoring functions are grouped into three main classes according to the methodology used to derive them. These three main approaches are generally termed force field based, knowledge based, and empirical.

Force field-based methods [9–11] mainly account for the binding energy between ligand and protein by evaluation of non-bonded interactions, i.e. coulombic and van der Waals potentials, between protein and ligand atoms. Such approaches have been very successful in simulating the microscopic behavior of biological molecules and complexes. Yet, such simulations require extensive sampling of possible protein–ligand poses, while, in general, only simple (i.e. static) force field approaches are viable for high-throughput screening in view of the computing time involved.

Knowledge-based potentials [12–18] are derived by collecting statistics on interatomic distances from a database of protein–ligand structures in order to determine potentials of mean force based on the probability of observing specific types of protein and ligand atoms at a given separation from each other.

Empirical scoring functions [19–27] consist of a set of terms characterizing various aspects of protein–ligand interactions such as energies of hydrogen bonding, steric interactions, lipophilic interactions, solvation, and entropic effects, and are therefore somewhat related to force-field based scoring functions. These descriptor terms are then usually combined into an overall scoring function by applying linear regression to the descriptor coefficients to fit binding affinity data of a set of protein–ligand complexes.

While all scoring function approaches have been successful to some extent in predicting experimental binding affinities, they all exhibit problems of varying degree in accurately and broadly scoring protein–ligand interactions. Various sources of inaccuracy can arise such as neglect of three-body and higher order effects by approximating atomic interactions as a sum of pair-wise terms, choices of atom types for protein and ligand atoms, and evaluation of the free energy of binding using a single static model of protein–ligand geometry for assessing free energy, which should more rigorously be a Boltzmann weighted average over all accessible conformations and poses. In addition, metal-containing systems often present a challenge for these models due to the nature of the interactions between a small molecule and a metal ion in the active site, e.g. partial covalent bonding, unusual hybridization states, etc.

In this work, we present the development of two new scoring functions termed *LigScore1* and *LigScore2* that have been trained across a broad set of protein–ligand complexes utilizing a methodology, namely genetic function approximation (GFA), that allows for the exploration of a wide variety of descriptors and equations resulting in two scoring functions that are simple, fast to calculate, and consist of physically reasonable terms and coefficients. *LigScore1* and *LigScore2* perform as well or better than many other more complex functions in terms of their fit to binding affinity data across a comparable training set. In addition, we show how the incorporation of a novel quadratic term identified by the GFA algorithm enabled the functions to fit a set of oligopeptide binding protein A (OppA) complexes which proved problematic for most other scoring functions. By avoiding issues associated with overfitting of the data and the use of physically interpretable and reasonable terms, the resulting scoring functions should prove useful in a variety of structure-based design applications. Finally, we compare their behavior with other popular scoring functions, analyze cases where the current functions prove deficient and suggest areas for future improvement and additional research.

2. Methods

2.1. Ligand–receptor complex preparation

We obtained crystal structures for ∼300 protein–ligand complexes from the Protein Data Bank with literature-known binding constant K_i values [19,22,23,25,28–30]. Upon removing problematic complexes from this set, we retained 122 complexes with an X-ray resolution of <2.5 Å (Table 1).

Missing residues and side chains that were not part of the active site were added and crystallographic waters were retained. Hydrogens were added using either Insight II [31] or Cerius^2 [32] according to the expected protonation state at experimental pH. Bond orders of all ligand molecules were also assigned. In the case of streptavidin–biotin complex (1STP), the streptavidin dimer was generated from symmetry aspects of the X-ray structure. To remove any unfavorable steric clashes and to optimize hydrogen-bonding patterns, the hydrogen atoms were subsequently minimized utilizing either the CFF force field parameter set [33–36] or the DREIDING force field parameters [37] in conjunction with Gasteiger charges [38]. For each set of force field parameters, 500 steps of smart minimization [32] were applied to each complex. Subsequently, all hydrogen-bonding patterns in the vicinity of the ligand-binding site were checked by visual inspection and corrected manually by torsional rotation of appropriate hydrogens. Complexes with corrected hydrogen bonds were again minimized with only hydrogens being flexible. Following this procedure, we obtained two coordinate sets of protein–ligand complexes (one for each force field) that were then used for training the *LigScore1* scoring function. After applying an additional 500 steps of minimization, during which the entire protein

Table 1
Protein–ligand complexes

Protein–ligand complex	PDB code	Exp. pK_i
Lysozyme(L99A)–benzene[b]	181L	3.76
Lysozyme(L99A)–benzofuran[b]	182L	3.95
Lysozyme(L99A)–indene[b]	183L	3.71
Lysozyme(L99A)–isobutylbenzene[b]	184L	4.71
Lysozyme(L99A)–indole[b]	185L	3.54
Lysozyme(L99A)–*n*-butylbenzene[b]	186L	4.84
Lysozyme(L99A)–*o*-xylene[b]	187L	3.37
Lysozyme(L99A)–*p*-xylene[b]	188L	3.33
Lysozyme(L99A)–benzene[b]	1L83	3.76
Lysozyme(L99A)–ethylbenzene[b]	1NHB	4.17
Arabinose-binding protein–α-L-arabinose[a]	1ABE-1	7.01
Arabinose-binding protein–β-L-arabinose[a]	1ABE-2	7.01
Arabinose-binding protein–α-D-fucose[a]	1ABF-1	5.42
Arabinose-binding protein–β-D-fucose[a]	1ABF-2	5.42
Arabinose-binding protein(P254G)–α-D-fucose[a]	1APB-1	5.82
Arabinose-binding protein(P254G)–β-D-fucose[a]	1APB-2	5.82
Arabinose-binding protein(P254G)–α-L-arabinose[a]	1BAP-1	6.85
Arabinose-binding protein(P254G)–β-L-arabinose[a]	1BAP-2	6.85
Glucose-binding protein–β-D-glucose[a]	2GBP	7.60
Arabinose-binding protein–α-D-galactose[a]	5ABP-1	6.64
Arabinose-binding protein–β-D-galactose[a]	5ABP-2	6.64
Arabinose-binding protein(M108L)–α-L-arabinose[a]	6ABP-1	6.36
Arabinose-binding protein(M108L)–β-L-arabinose[a]	6ABP-2	6.36
Arabinose-binding protein(M108L)–α-D-fucose[a]	7ABP-1	6.46
Arabinose-binding protein(M108L)–β-D-fucose[a]	7ABP-2	6.46
Arabinose-binding protein(M108L)–α-D-galactose[b]	8ABP-1	8.00
Arabinose-binding protein(M108L)–β-D-galactose[b]	8ABP-2	8.00
Arabinose-binding protein(P254G)–α-D-galactose[b]	9ABP-1	8.00
Arabinose-binding protein(P254G)–β-D-galactose[b]	9ABP-2	8.00
Oligo-peptide binding protein A–Lys-Cys-Lys[a]	1B05	7.13
Oligo-peptide binding protein A–Lys-Nap-Lys[a]	1B0H	6.70
Oligo-peptide binding protein A–Lys-Hph-Lys[a]	1B1H	7.03
Oligo-peptide binding protein A–Lys-Orn-Lys[a]	1B2H	4.54
Oligo-peptide binding protein A–Lys-Gly-Lys[a]	1B31	5.89
Oligo-peptide binding protein A–Lys-Met-Lys[a]	1B32	7.10
Oligo-peptide binding protein A–Lys-His-Lys[a]	1B3F	6.89
Oligo-peptide binding protein A–Lys-Ile-Lys[a]	1B3G	6.70
Oligo-peptide binding protein A–Lys-Chx-Lys[a]	1B3H	6.21
Oligo-peptide binding protein A–Lys-Phe-Lys[a]	1B40	7.28
Oligo-peptide binding protein A–Lys-Pro-Lys[b]	1B46	5.28
Oligo-peptide binding protein A–Lys-Dab-Lys[a]	1B4H	5.46
Oligo-peptide binding protein A–Lys-Asp-Lys[a]	1B4Z	5.23
Oligo-peptide binding protein A–Lys-Ser-Lys[b]	1B51	7.37
Oligo-peptide binding protein A–Lys-Tyr-Lys[a]	1B58	6.59
Oligo-peptide binding protein A–Lys-Dap-Lys[a]	1B5H	6.01
Oligo-peptide binding protein A–Lys-Asn-Lys[a]	1B5I	7.05
Oligo-peptide binding protein A–Lys-Gln-Lys[b]	1B5J	7.43
Oligo-peptide binding protein A–Lys-Nva-Lys[a]	1B6H	7.82
Oligo-peptide binding protein A–Lys-Nle-Lys[a]	1B7H	8.02
Oligo-peptide binding protein A–Lys-Leu-Lys[a]	1B9J	5.96
Oligo-peptide binding protein A–Lys-Ala-Lys[a]	1JET	7.25
Oligo-peptide binding protein A–Lys-Glu-Lys[b]	1JEU	6.82
Oligo-peptide binding protein A–Lys-Trp-Lys[a]	1JEV	6.89
Oligo-peptide binding protein A–Lys-Arg-Lys[b]	1QKA	5.92
Oligo-peptide binding protein A–Lys-Val-Lys[a]	1QKB	7.35
Oligo-peptide binding protein A–Lys-Lys-Lys[a]	2OLB	5.54
HIV protease–hydroxyethylene	1AAQ	8.40
HIV protease–A79285	1DIF	10.66
HIV protease–SB203238	1HBV	6.37
HIV protease–CPG53820	1HIH	8.53
HIV protease–SB204144	1HOS	8.55
HIV protease–SB206343	1HPS-1	9.22
HIV protease–SB206343	1HPS-2	9.22
HIV protease–VX478	1HPV	9.22
HIV protease–KNI272	1HPX	8.22
HIV protease–L735524	1HSG	9.42
HIV protease–GR123976	1HTE	7.00
HIV protease–GR126045	1HTF-1	8.09
HIV protease–GR126045	1HTF-2	8.09
HIV protease–GR137615	1HTG-1	9.68
HIV protease–GR137615	1HTG-2	9.68
HIV protease–(R,S)-A77003[a]	1HVI	10.10
HIV protease–(S,-)-A78791[a]	1HVJ	10.50
HIV protease–(S,S)-A76928[a]	1HVK	10.11
HIV protease–(R,R)-A76899[a]	1HVL	9.00
HIV protease–XK263	1HVR	9.51
HIV protease(V82A)–A77003	1HVS	10.08
HIV protease–A9888	1PRO	11.30
HIV protease–SB203386	1SBG	7.74
HIV protease–U100313	2UPJ	10.39
HIV protease–MTV101	4HVP	6.11
HIV protease–L700,417[a]	4PHV-1	9.15
HIV protease–L700,417[a]	4PHV-2	9.15
HIV protease–acetylpepstatin	5HVP-1	7.46
HIV protease–acetylpepstatin	5HVP-2	7.46
HIV protease–JG365	7HVP	9.62
HIV protease–U85548E	8HVP	9.00
HIV protease–A74704	9HVP	8.35
Trypsin(D189G,G226D)–benzamidine	1BRA	1.82
Thrombin–benzamidine	1DWB	2.90
Thrombin–argatroban	1DWC	7.41
Thrombin–Napap	1DWD	8.18
Elastase–Tfa-Lys-Pro-Iso[a]	1ELA	6.66
Elastase–Tfa-Lys-Leu-Iso[b]	1ELB	7.16
Elastase–Tfa-Lys-Phe-Iso[b]	1ELC	6.36
Thrombin–Mqpa[a]	1ETR	7.72
Thrombin–Napap	1ETS	8.22
Thrombin–Tapap	1ETT	5.89
Trypsin–Napap	1PPC	6.16
Trypsin–3-Tapap	1PPH	5.92
Trypsin–aminomethylcyclohexane[b]	1TNG	2.93
Trypsin–4-fluorobenzylamine	1TNH	3.37
Trypsin–4-phenylbutylamine[b]	1TNI	1.70
Trypsin–2-phenylethylamine	1TNJ	1.96
Trypsin–3-phenylpropylamine	1TNK	1.49
Trypsin–t-2-phenylcyclopropylamine[b]	1TNL	1.88
Trypsin–benzamidine[a]	3PTB	4.92
Elastase–Tfa-Leu-Ala-P-trifluoromethylphenylanilide	7EST	7.60
Carboxypeptidase A–L-benzylsuccinate[b]	1CPX	6.35
Carboxypeptidase A–sulfoiimine[b]	1CPS	5.56
Carboxypeptidase A–L-phenylacetate[a]	2CTC	3.89
Carboxypeptidase A–Gly-L-Tyr[b]	3CPA	3.88
Thermolysin–*N*-(1-carboxy-3-phenyl)-L-Leu-Trp[b]	1TMN	7.30
Thermolysin–Val-Trp[a]	3TMN	5.90
Penicillopepsin–Iva-Val-Val-LySta-O-Et[b]	1ATP	9.39
FK506-binding protein–FK506[a]	1FKF	9.70
Cytochrome P450–metyrapone	1PHG	8.66
Retinol-binding protein–retinol[b]	1RBP	6.72
Sulfate-binding protein–sulfate[b]	1SBP	6.92
Streptavidin–biotin	1STP	13.40
Immunoglobulin–GAS[b]	2CGR	7.27
Dihydrofolatereductase–methotrexate[a]	4DFR	9.70

[a] Training set for *LigScore1* (50 complexes).
[b] Test set for *LigScore1* (32 complexes).

was constrained and only the ligands moved, two more coordinate sets for each protein–ligand complex were derived, against which the *LigScore2* scoring function was trained. Since some of the ligands displayed rather large movements in the final minimization (RMS deviations larger than 1.5 Å), the minimization of those ligands was repeated starting from the cleaned-up and hydrogen-minimized structure with all ligand atoms restrained by a harmonic force of 0.25 kcal/(mol Å^2). In the case of CFF force field, the ligands of 1TNI, 1TNL and 3CPA needed to be restrained, while for Gasteiger/DREIDING only 1TNI needed restraining.

2.2. Soft van der Waals descriptor

The van der Waals (vdW) energy of protein–ligand interactions is computed via a Lennard–Jones 9–6 potential [39] using van der Waals radii and energy parameters of either the CFF [33–36] or the DREIDING [37] force field. Since the 9–6 potential will overly penalize 'mild' short contacts between ligand and protein atoms, we soften the potential so that it gradually rises to a large but finite value at zero separation between atoms as suggested by Levitt [40]:

$$\langle E_{\mathrm{vdW}} \rangle = \sum_{\substack{i \in \text{ligand} \\ j \in \text{protein}}} \frac{\varepsilon_{ij}\left[2\left[\left(\frac{r^*_{ij}}{r_{ij}}\right)^9\right] - 3\left[\left(\frac{r^*_{ij}}{r_{ij}}\right)^6\right]\right]}{2\sqrt{\varepsilon_j}\left(\frac{\sqrt{r^*_j}}{r_{ij}}\right)^9 \alpha(1+\beta r^2_{ij}) + 1} \quad (1)$$

where $\varepsilon_{ij} = \sqrt{\varepsilon_i \varepsilon_j}$, $r^*_{ij} = \sqrt{r^*_i r^*_j}$, α and β are parameters that control the value of the function at $r_{ij} = 0$ as well as the rate at which the function approaches the maximum value at zero separation, respectively. Our modified form of the Levitt function enables us to employ a protein-based energy grid that incorporates the contributions of all protein atoms independently of all ligand atoms. For this particular van der Waals interaction, its value at $r_{ij} = 0$ depends on the values of the ligand atom parameters, ε_i and r^*_i. In the *LigScore* functions, α is set to $1\sqrt{\text{mol/kcal Å}^9}$ and β to 0.05 Å^{-2}.

2.3. Surface descriptor calculation

For each ligand atom we uniformly distribute 500 surface points on a van der Waals radius sphere centered at the given atom. Of the 500 surface points of each ligand atom, the ones that are not enclosed by the vdW sphere of any other ligand atom are "exposed". Since only "exposed" surface points are considered for calculating any *LigScore* surface descriptors, we will hence refer to them simply as surface points.

In the next step, we define a uniform 0.25 Å grid that encloses the user-defined active site of the ligand–receptor complexes. This grid extends 5 Å in each direction beyond the binding site. Each site grid point is assigned to the closest protein atom if the coordinates of the grid point lie within a distance of 1.5 times the vdW radius of the center of that particular protein atom. All ligand surface points are then partitioned into either being in contact or not being in contact with any protein atom. A ligand surface point is considered to be in contact with a protein atom, if the nearest site grid point is assigned to a protein atom. Any surface point not in contact with any protein atom is considered to be solvent accessible. Consequently, while each surface point is always associated with a ligand atom, only some of them may be in contact with a protein atom as well. Based on the polarity of the associated ligand atom, a surface point is classified as either polar or non-polar.

We employ two different schemes in determining the polarity of an atom. The first one is based on the partial charge that the atom is assigned. Partial charges are either calculated using the Gasteiger charge algorithm [38] or obtained from the CFF force field parameters. Atoms possessing an absolute Gasteiger charge >0.15 or an absolute CFF charge >0.20 are considered to be polar. For this partial charge-based polarity assignment, it was found that in some cases small perturbations in the chemical environment of an atom would unexpectedly alter its polarity assignment and would lead to degraded results in the fitting of the scoring function. For this reason, in the case of the *LigScore2* function, we switched to an atom-type based approach to determine the polarity of an atom (see Table 2). The typing rules were developed based on observing the polarity patterns found in most ligands using either the Gasteiger or CFF charges. In both schemes, atoms are classified as being positive polar, negative polar or non-polar. In addition, we considered surface contacts involving ionic species and also metals based on the existence of a formal atom charge (ionic) or element type (metal), respectively.

Contacts between positive polar and negative polar atoms are classified as attractive contacts, while positive-positive and negative-negative atom contacts are classified as repulsive. A given surface descriptor is then obtained by summing all appropriate surface points weighted by their fractional surface area. Table 3 summarizes all the surface descriptors that were considered for devising a new scoring function.

Table 2
Atom types

Element	Atom properties	Atom polarity
H	Bonded to O or N	Positive
C	Carbonyl carbon	Positive
O		Negative
N		Negative
N	Positive formal charge, guanidium	Positive
S, P	Bonded to four atoms	Positive
S, P	Not bonded to four atoms	Negative
F, Cl, Br, I		Negative
Metal ions		Positive
All others		Non-polar

2.4. Genetic algorithm scheme

The *LigScore* scoring functions have been developed by employing the genetic function approximation [41,42] as follows. First, the entire descriptor set (a total of more than 50 descriptors including those listed in Table 3 and various descriptors concerning van der Waals, classical electrostatic, ligand strain energies as well as number of rotatable torsion angles) was fed through a genetic algorithm using a least-squares regression approach to fit different subsets of descriptors to experimental pK_i values. In this process a set of 100 equations was evolved for 10,000 generations of the genetic algorithm, while considering both linear and quadratic descriptor terms. The length of each equation was initially set to four terms including a constant term. During the genetic evolution of these equations the following operations were permitted with a 50% probability for each step of the genetic algorithm: adding a new term, reducing, or extending the equation [41]. Subsequently, a set of 100 additional equations without a constant term was generated utilizing the same protocol. The following selection criteria were then applied to the 200 resulting equations in order to select a new scoring function: the scoring function had to display an r^2 larger than 0.70 as well as consisting of three to four physically reasonable descriptors entering with the correct sign. Different subsets of the full training set were also tested in order to avoid bias towards a particular protein family. The resulting set of equations was then inspected for the most frequently occurring descriptors. A common subset of three key descriptors (vdW and two surface descriptors) were thus identified. In order to refine the model further, outliers with a deviation larger than 2.5 pK_i units were removed from the original training set. A multiple linear regression on this revised training set with these three descriptors yielded a preliminary scoring function. Starting from this preliminary function a manual ''leave-one-out'' and/or ''add-one'' scheme that covered the entire descriptor space resulted in the final scoring equation with a maximal r^2 value.

Table 3
Surface descriptors

Descriptor	Type
Cneg_pol_pol	Repulsive protein/ligand polar surface contact
Cneg_ion_ion	Repulsive protein/ligand ionic surface contact
Cneg_pol_ion	Repulsive protein/ligand polar-ionic surface contact
Cneg_met_pol	Repulsive protein/ligand metal-polar surface contact
Cneg_met_ion	Repulsive protein/ligand metal-ionic surface contact
Cneg_tot	Sum of repulsive protein/ligand surface contacts
Cpos_pol_pol	Attractive protein/ligand polar surface contact
Cpos_ion_ion	Attractive protein/ligand ionic surface contact
Cpos_pol_ion	Attractive protein/ligand polar-ionic surface contact
Cpos_met_pol	Attractive protein/ligand metal-polar surface contact
Cpos_met_ion	Attractive protein/ligand metal-ionic surface contact
Cpos_tot	Sum of attractive protein/ligand surface contacts
Cpol_lip	Polar/non-polar protein/ligand surface contact
Cion_lip	Ionic/non-polar protein/ligand surface contact
Cmet_lip	Metal/non-polar protein/ligand surface contact
Clip_lip	Non-polar protein/ligand surface contact
Bulk_pol_lig	Polar ligand surface accessible to solvent
Bulk_ion_lig	Ionic ligand surface accessible to solvent
Bulk_pol_lig	Non-polar ligand surface accessible to solvent
Bury_lip_lig	Buried non-polar ligand surface
Bury_pol_lig	Buried polar ligand surface
Bury_ion_lig	Buried ionic ligand surface
Bury_tot_lig	Sum of buried ligand surface

3. Results and discussion

LigScore1 has been developed utilizing the above protocol trained against a set of 50 protein–ligand complexes and tested against an additional set of 32 complexes (see Table 1) obtained from high resolution X-ray structures, whose experimental binding affinities range from pK_i = 1.49–13.4. Early on, the vdW energy term $\langle E_{vdW} \rangle$ was present in most equations returned by the GFA. Subsequent selection of others descriptors was therefore driven by incorporating energy terms that represent electrostatics and solvation effects. The final functional form of *LigScore1* is simple and contains only three descriptors:

$$pK_i = C - \beta_1 \langle E_{vdW} \rangle + \beta_2 \text{Cpos\_tot} - \beta_3 \text{TotPol}^2 \quad (2)$$

where $\langle\ \rangle$ indicates the summation of all interactions between the ligand and protein atoms. Cpos_tot is the total surface area of the ligand involved in attractive polar interactions with the protein, and TotPol^2 is equal to Cpos_tot^2 + Cneg_tot^2, where Cneg_tot is the total surface area of the ligand involved in repulsive polar interactions with the protein. The overall fit of *LigScore1* with experimental pK_i's is shown in Fig. 1 and possesses a correlation coefficient, r^2, of 0.79 with a standard deviation, s_{dev}, of 0.70, whereas the combination of the training and test set (82 complexes) possesses an s_{dev} of 1.40. Since Cpos_tot and TotPol^2 are always positive, the first term in *LigScore1* characterizes favorable protein–ligand electrostatics, while the latter represents a desolvation penalty that is paid when the ligand binds to the protein. The simplicity of this equation and good correlation with experimental binding constants is all the more remarkable as it covers protein complexes with differently sized binding pockets and very distinct binding modes. In particular, the affinities of the OppA complexes, which we have found to be consistently overestimated by many other scoring functions such as *Ludi*, *PLP*, or *Jain* [19–22,43], were predicted correctly by *LigScore1*. Despite its good correlation with most of the protein classes, the lysozyme protein complexes with millimolar binding affinities were consistently underestimated by *LigScore1* (Fig. 1). This result lead us to reconsider the desolvation penalty term TotPol^2 in *LigScore1*. It displays a quadratic dependence on the polar contact surfaces between ligand and protein atoms that is similar to the functional charge-dependence of the desolvation penalty of a point charge, q, inside a spherical dielectric medium [44]. However, it is not in a form that can be readily

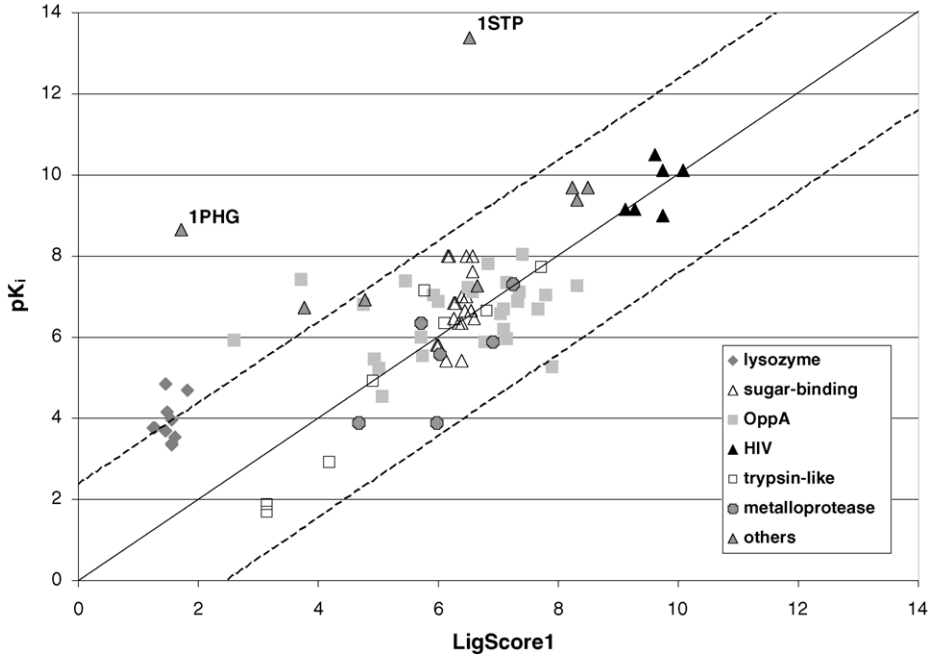

Fig. 1. The plot of experimental pK_i against computed *LigScore1* for 84 protein–ligand complexes from X-ray structures. This includes 32 complexes that the scoring function was tested against, and two extreme outliers (1PHG, 1STP) that were not included in either the testing or training of *LigScore1*. The dashed lines indicate the 2.5 pK_i cutoff used to determine "outliers" in the model.

partitioned into the contributions from the ligand or the protein, respectively. Nevertheless, one would expect that contributions to the desolvation penalty from the protein should primarily depend on the loss of interactions with waters being replaced by the bound ligand, and not on newly established interactions between ligand and protein, which are already mainly accounted for in the $\langle E_{vdW} \rangle$ and Cpos_tot terms. A new solvation penalty descriptor should therefore consist of symmetrical contributions from the ligand as well as the protein. Inspiration for this new descriptor was drawn from a particular OppA protein complex named 1JEV. In this protein–ligand complex, water molecules previously bound to polar regions in the OppA binding site are replaced by the tripeptide ligand, Lys-Trp-Lys. The TotPol^2 term of *LigScore1* does not account for the desolvation of all protein atoms in this complex, because it ignores various contacts of polar protein atoms with non-polar ligand atoms of 1JEV, which replace buried waters. A more plausible protein desolvation descriptor should account for the entire desolvated polar protein surface, which occurs upon removal of waters resulting in the polar protein surface being buried upon binding with the ligand.

On the other hand, the same argument would hold for a polar portion of the ligand binding to a lipophilic protein-binding site. Hence, we examined protein–ligand surface descriptors of the following form:

$$\text{SolvPlty\_lig}^2 = (\text{Bury\_tot\_lig} - \text{Bury\_lip\_lig})^2$$
$$\text{SolvPlty\_prot}^2 = (\text{Cpos\_tot} + \text{Cneg\_tot} + \text{Bury\_lip\_lig} - \text{Clip\_lip})^2$$

as a replacement for TotPol^2 in *LigScore1*. The first term represents the overall polar ligand surface that is buried inside the protein-binding site, while the second term indirectly accounts for the polar protein surface in contact with the bound ligand molecule. The polarity of all atoms was now based on atom types (see Table 2) rather than partial atom charges, as was done in *LigScore1*, for reasons mentioned above in the discussion under Section 2.3.

This eliminated the charge threshold parameter, which governed whether an atom is considered polar or non-polar. Nonetheless, polar contact surface descriptors that are based on atom types correlated well with our previously employed charge-based ones as displayed for Cpos_tot in Fig. 2 ($r^2 = 0.99$). Adding the two new descriptors to our "genetic algorithm scheme", resulted in a new and enhanced *LigScore2* equation:

$$\text{p}K_i = C - \beta_1 \langle E_{vdW} \rangle + \beta_2 \text{Cpos\_tot} - \beta_3 (\text{SolvPlty\_lig}^2 + \text{SolvPlty\_prot}^2)$$

with an r^2 of 0.74 and an s_{dev} of 1.04 for an enlarged training set of 112 complexes (Fig. 3) excluding 10 outliers (1AAQ, 1BRA, 1ELB, 1ELC, 5HVP-1, 5HVP-2, 8HVP, 1PHG, 1STP, 1TNK) from the training. It should be pointed out that, in principle, our previous set of descriptors should have been sufficient to lead us to *LigScore2* when subjecting them to the GFA algorithm. However, the complex functional dependence with regard to our initial set of descriptors would have required the length of the equation to consist of 15 terms. Starting from an initial length of four descriptors,

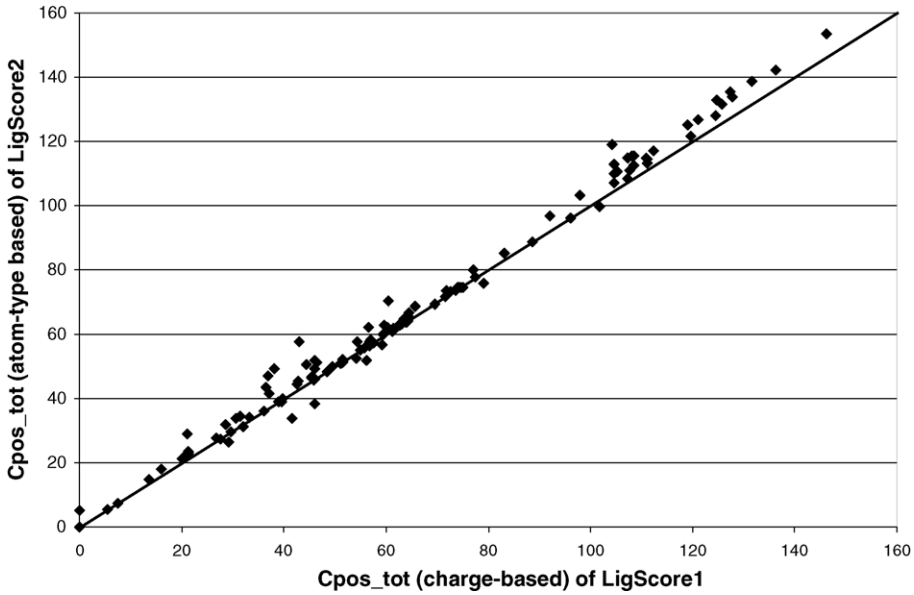

Fig. 2. A plot comparing attractive polar surface area (Cpos_tot) of contact between ligand and protein obtained using two methods for identifying polar atoms. The *y*-axis corresponds to the *LigScore2* Cpos_tot value obtained with polar atoms identified using atom types (see Table 2), while the *x*-axis corresponds to Cpos_tot with polar atoms identified by the charge on the atom as in *LigScore1*.

the GFA algorithm was unable to arrive at the final *LigScore2* function, because the *Lack of Fit* function used in the GFA algorithm penalizes functions with too many terms. By consolidating the multiple descriptors into a single descriptor (which still corresponds to a term amenable to simple physical interpretation), we essentially ''assisted'' the GFA algorithm to arrive at the improved answer.

Although a slightly better correlation with experimental data could have been achieved by separating SolvPlty_lig[2] and SolvPlty_prot[2] into two independent terms, considering the equal physical importance and meaning of both terms, we chose to consolidate them into one desolvation penalty term with a single regression coefficient. The lysozyme complexes were now in good agreement with the predicted pK_i values of *LigScore2*. Nevertheless, some extreme outliers were observed for *LigScore2*, in particular the two 5HVP complexes with pK_i differences of 7 and 4.5 between the experimental and predicted binding affinities

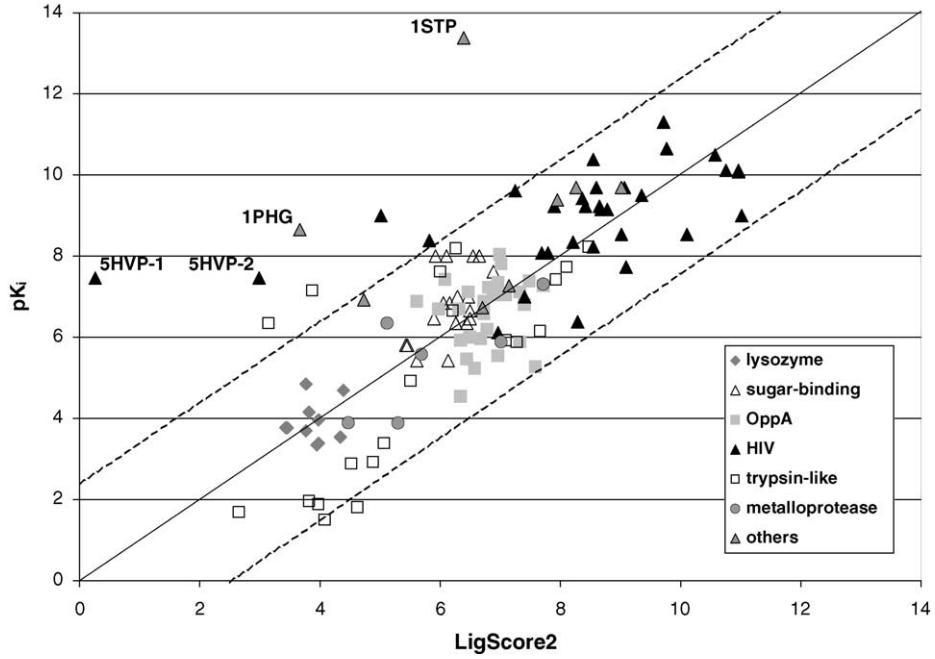

Fig. 3. The plot of experimental pK_i against computed *LigScore2* for 122 protein–ligand complexes from X-ray structures. The dashed lines indicate the 2.5 pK_i cutoff used to determine ''outliers'' in the model.

(Fig. 3), respectively. This result was somewhat surprising because 5HVP belongs to the HIV protease complexes, and *LigScore2* predicted the pK_i's of all other HIV protease complexes extremely well. A closer examination of 5HVP and its individual contributions of $\langle E_{vdW} \rangle$, Cpos_tot, and SolvPlty[2] to *LigScore2* revealed that 5HVP possessed rather large unfavorable vdW contacts between several ligand and protein atoms. Some of the protein–ligand heavy atom distances for 5HVP were <2 Å. In order to relieve such strong vdW repulsions, the ligands were consequently minimized with the protein atoms constrained to their X-ray positions. In some instances, a small harmonic restraining force was placed on the ligand atoms to prevent them from drifting too far from their original X-ray location. The correlation coefficient, r^2, of the refitted *LigScore2* equation significantly improved from 0.56 to 0.75 for the expanded data set of 118 with a reduction of the s_{dev} value from 1.43 to 1.04 (Fig. 4). In addition, the number of outliers decreased to 4 consisting of 1BRA, 1PHG, 1SBP, and 1STP. A summary of the coefficients of all *LigScore* equations and their statistics is provided in Table 4.

Since *Ligscore1* and *LigScore2* were developed with different training sets, comparing their performance on an identical data set of 122 complexes is shown in Fig. 5 demonstrating the improvement of *LigScore2* over *LigScore1*.

The following cross validation study was performed to evaluate the robustness and predictive power of the *LigScore2* equation. In this study, 10 separate trials were performed, in which the data set of 118 complexes was randomly divided into a training and test set of 59 complexes each. The *LigScore2* equation was then fitted each time against the new training set, and the pK_i values of the test set were predicted with this new *LigScore2* equation. The final averaged correlation coefficient, r^2, equaled 0.73 with a s_{dev} value of 1.08, while the averaged predictive correlation coefficient, q^2, was 0.71 with a standard deviation of the error of prediction, s_{press}, of 1.11. The absence of any dramatic change in r^2 and q^2 clearly demonstrates the self-consistency and robustness of the *LigScore2* equation.

Surprisingly, various forms of an electrostatic potential were not picked up by the GFA algorithm. This includes screening the protein–ligand interactions by increasing the dielectric constant or allowing for a distance-dependent dielectric parameter. Even separating the attractive from the repulsive parts of the potential, as suggested by the attractive polar surface descriptors of the *LigScore* equations, did not yield electrostatic potential descriptors that correlate well with the experimental binding affinities. Other forms of hybrid-like surface-weighted electrostatic energy terms were also not selected by the GFA as part of the scoring function. The results seem to suggest that the long-range contributions of a $1/r$-dependent potential (or related forms) do not correlate well with the experimental data.

Since this finding might be considered an artifact of the underlying force field parameter set, we derived equivalent *LigScore1* as well as *LigScore2* equations for two different force fields, utilizing either the CFF force field [33–36] or a combined set of Gasteiger charges [38] and DREIDING parameters [38]. It should be pointed out that charge

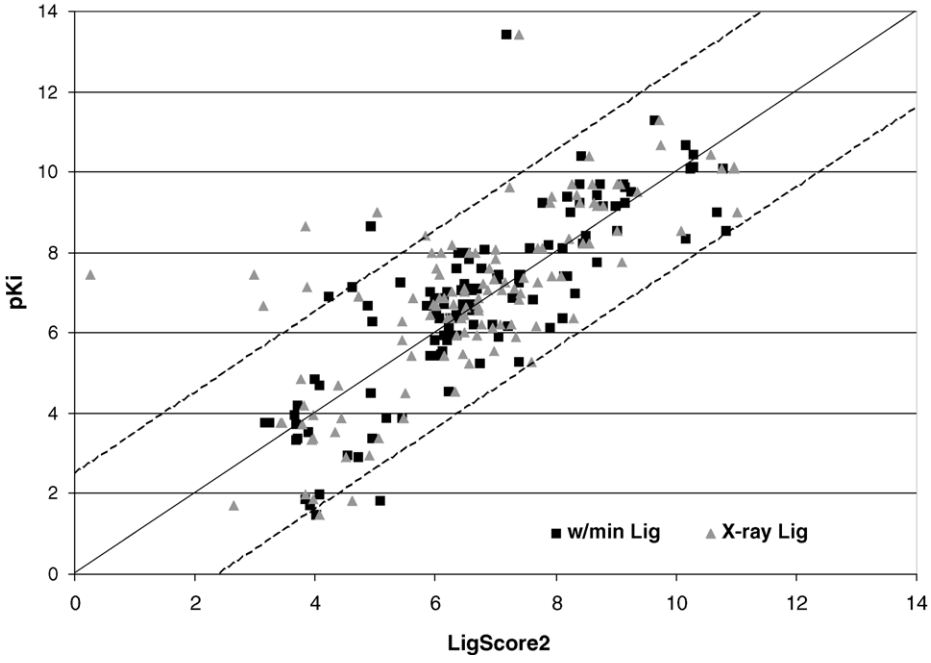

Fig. 4. The plot of experimental pK_i against computed *LigScore2* for 122 protein–ligand complexes. This plot shows the computed *LigScore2* for X-ray as well as for energy-minimized ligand poses. The ligand poses were energy minimized with protein atoms fixed and in some cases with ligand atoms restrained using a harmonic constraint to keep them from moving too far from the X-ray locations. The dashed lines indicate the 2.5 pK_i cutoff used to determine "outliers" in the model.

Table 4
Summary of *LigScore* equations

	C	β_1	β_2	β_3	# Train compls	r^2	s_{dev}	F	q^2
LigScore1 [Soft,CFF]	0.489646	0.045508	0.143912	0.00100980	50	0.79	0.70	57.2	0.76
Ligscore1 [Grid,CFF]	0.517527	0.043650	0.143901	0.00099039	50	0.79	0.69	59.2	0.76
LigScore1 [Soft,Dreid/Gast]	0.349774	0.046731	0.165259	0.0011323	50	0.77	0.73	51.7	0.73
LigScore1 [Grid,Dreid/Gast]	0.317636	0.045166	0.164671	0.0011164	50	0.77	0.72	52.7	0.74
LigScore2 (xray) [Soft,CFF]	2.07512	0.080275	0.064145	0.000088388	112	0.74	1.06	103.2	0.72
LigScore2 (xray) [Grid,CFF]	2.26476	0.072865	0.062176	0.000081525	112	0.74	1.08	99.6	0.72
LigScore2 (xray) [Soft,Dreid]	1.97433	0.081007	0.065186	0.000085975	112	0.73	1.09	97.2	0.71
LigScore2 (xray) [Grid,Dreid]	2.12468	0.075016	0.063048	0.000081110	112	0.73	1.09	95.1	0.71
LigScore2 (min) [Soft,CFF]	1.90018	0.072975	0.062458	0.000073235	118	0.75	1.04	112.0	0.73
LigScore2 (min) [Grid,CFF]	2.14158	0.066256	0.061882	0.000069032	118	0.74	1.09	105.7	0.72
LigScore2 (min) [Soft,Dreid]	1.53863	0.076224	0.065007	0.000078209	118	0.72	1.13	95.2	0.70
LigScore2 (min) [Grid,Dreid]	1.77294	0.070711	0.063160	0.000074003	118	0.71	1.15	90.7	0.69

Soft: softened Lennard–Jones potential of Eq. (1); Grid: grid-based approximation of softened Lennard–Jones potential [39]; CFF: CFF force field [33–35]; Dreid/Gast: DREIDING force field [37] in combination with Gasteiger charges [38]; xray: original PDB X-ray structure of protein–ligand complex with minimized hydrogens; min: PDB protein–ligand complexes with ligands minimized in presence of constraint proteins; F: F-value; q^2: predictive ''leave-one-out'' r^2. *LigScore1* [Soft,CFF], *LigScore2* (xray) [Soft,CFF], and *LigScore2* (min) [Soft,CFF] are the versions of the scoring equations that are mainly referred to in figures, tables and text of this article.

dependency only enters in the *LigScore1* equation via a charge threshold, above which an atom is consider to be polar. Nevertheless, replacing this criterion in *LigScore2* with atom-type rules for polarity altered the polar contact descriptor only slightly (Fig. 2) and eliminated any charge dependency. Consequently, neither equation exhibits a continuous functional dependence with regard to interacting atomic charges, as one would expect from descriptors resembling electrostatic forces. Current efforts are therefore underway to replace this polar contact term with a descriptor that has an explicit dependence on atomic charges.

Efforts to incorporate a term accounting for entropy, such as the number of rotatable bonds of the ligand, did not result in a significant improvement in the fit and sometimes the resulting fit showed the rotatable bond count term with the wrong sign. Similarly, attempts to incorporate a term accounting for ligand strain energy difference upon binding were also unsuccessful.

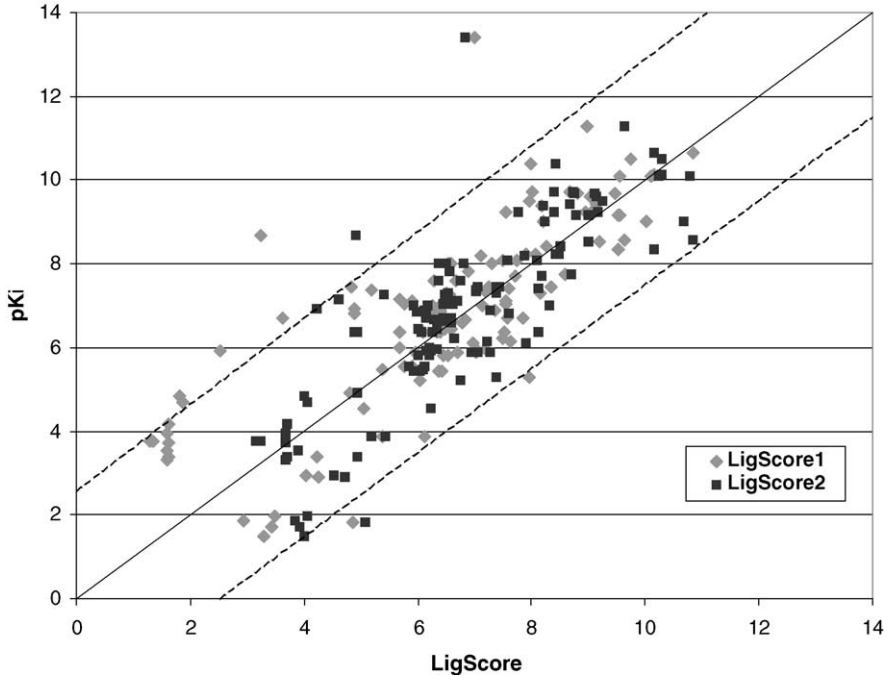

Fig. 5. The plot of experimental pK_i against computed *LigScore1*/*LigScore2* for 122 protein–ligand complexes. This plot displays the computed *LigScore1* and *LigScore2* scores for the same set of 122 complexes with energy-minimized ligand poses. The dashed lines indicate the 2.5 pK_i cutoff used to determine ''outliers'' in the model. For the entire 122 data points, the r^2 for *LigScore1* and *LigScore2*, respectively, are 0.60 and 0.65 and the corresponding s_{dev} are, respectively, 1.50 and 1.29 log units. If the four *LigScore2* outliers are ignored, the r^2 for *LigScore1* and *LigScore2*, respectively, are 0.69 and 0.75 and s_{dev} are, respectively, 1.28 and 1.04 log units. This demonstrates the improvement of *LigScore2* over *LigScore1* for this particular dataset.

Table 5
Comparison of scoring functions

Scoring function	LUDI-SCORE2	VALIDATE	DOCK	ChemScore	*X*-Score	PMF	*LigScore1*	*LigScore2* (min)
# Compls	82	51	103	82	170	65	80	118
# Parameters	8	13	8	5	11	1	4	4
r^2	0.79	0.85	0.70	0.71	0.78	0.77	0.74	0.75
s_{dev}	1.28	1.02	1.32	1.40	1.16	1.34	1.06	1.04
F	40.3	17.8	32.3	47.1	55.4	210.9	104.2	112.0
q^2		0.78	0.65	0.66	0.74		0.72	0.73
s_{press}		1.13		1.52	1.10		1.07	1.10

Parameters: number of adjustable parameters in scoring equation including a constant term; s_{press}: standard deviation of the error of prediction.

Future enhancements of our scoring function work may therefore need to address the following contributions to the binding affinity energy: intramolecular forces, entropic effects, ionic strength/pH of the solvent, binding of co-substrates and/or ions.

However, the current form of the *LigScore* functions already seem sufficiently accurate to be employed using in silico high-throughput docking/scoring experiments as exemplified by an enrichment study for thymidine kinase (1KIM), where a set of 1002 molecules containing nine known thymidine kinase inhibitors was previously docked employing the *LigandFit* docking program (see ref. [39] for more details). Since energy minimization of the ligands in the protein site improved the fitting of *LigScore2* to the pK_i experimental data (Fig. 4), it was of interest to study the effect of ligand energy minimization on the hit rate plot for this system. As can be seen in Fig. 6, docking and minimizing the ligands in the protein receptor site clearly leads to a significantly improved recovery of active versus random ligands using *LigScore2*.

When compared with other empirical scoring functions, as seen in Table 5, both *LigScore* functions stand out, since they possess a comparable correlation coefficient, r^2, and smaller standard deviation, yet contain only four adjustable parameters and span a training set of diverse proteins. Allowing for only a small ratio of descriptor terms versus the number of protein–ligand complexes should help to avoid the potential pitfall of overfitting the experimental data.

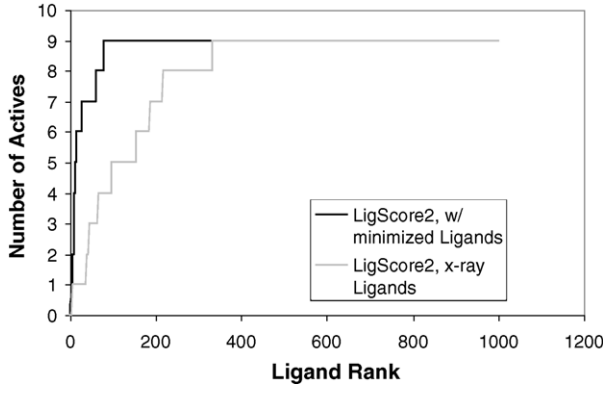

Fig. 6. A hit rate plot showing the ranks of nine known active compounds among a total of 1002 compounds docked into thymidine kinase receptor.

Table 6
Experimental and calculated pK_i values for ligands of avidin [46]

Ligand	pK_i	*LigScore1*	*LigScore2*
Biotin	14.89	6.87	7.17
4-Methyl-imidazolidone	4.47	4.65	4.88
Hexanoic acid	2.52	3.12	4.12

Despite the successful prediction of experimental affinities, a closer look at a few of the common outliers of *LigScore1* and *LigScore2* is warranted. Biotin-streptavidin (1STP) is among the pico-molar outliers that highlight the difficulty in working with some of the experimental data. In this case, the experimental assay used in determining the binding inhibition constant K_i display a biphasic decay, yielding a fast and slow dissociation rate. Since the slow dissociation off-rate is on the order of months, the K_i error is quite large. In addition, the dual nature of the dissociation seems to reveal a more complex binding process that is different than a simple two-body dissociation equilibrium. For instance, binding studies on a streptavidin-homologous protein revealed that the sum of the pK_i's of two compounds is significantly smaller than the pK_i of biotin itself (see Table 6), although combined they are chemically equivalent to biotin and bind correspondingly to the protein. A metastable intermediate state might, therefore, exist along the dissociation pathway of biotin that is missing for the other two molecules, whose binding affinities both *LigScore1* as well as *LigScore2* predict fairly well. It is free-energy gain from the intermediate to the bound state that both scoring functions are unable to capture. The corresponding increase in pK_i can likely be attributed to energetically favorable changes in the protein structure enhancing the hydrogen bonds between the imidazolidone group and the protein.

4. Summary

We have developed two new empirical scoring functions termed *LigScore1* and *LigScore2* that not only reliably predict binding affinities between ligand molecules and their protein receptors, but are also suitable for in silico high-throughput screening of large numbers of compounds against a therapeutic protein target. While consisting of only

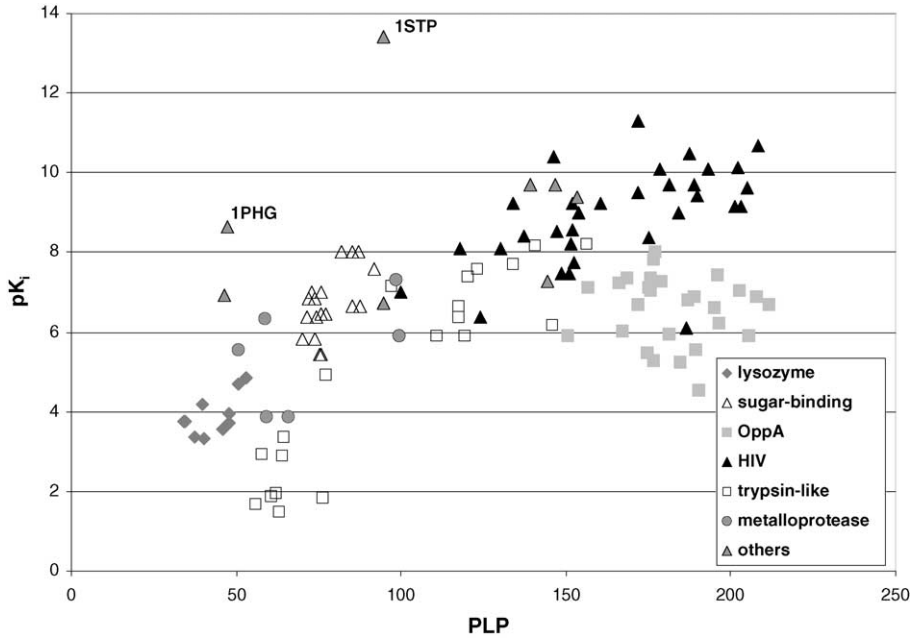

Fig. 7. The plot of experimental pK_i against computed *PLP* score [20] for 122 protein–ligand complexes from X-ray structures. The OppA as well as some of the trypsin complexes are clearly overestimated with regard to *PLP* scores.

three simple energy-related descriptors that were selected on grounds of physical intuition, these functions are capable of evaluating protein–ligand affinities in milliseconds per 3D protein–ligand structure on modern computer hardware. On a 2.4 GHz Xeon Pentium PC, computation of *LigScore1* or *LigScore2* functions using the grid-based vdW energy takes about 20 ms per molecule for a protein with 4630 atoms and a ligand with a molecular weight of around 320. The one-time energy grid computation for this protein takes about 2 min.

One of the three descriptors is a modified Lennard–Jones potential that accounts for the short-range repulsions as well as long-range attractive dispersion forces between ligand and protein atoms. The other two terms are based on contact surface areas determined by overlap of van der Waals sphere representations of the bound ligand and the protein receptor. One of them, the attractive polar contact surface, equals the surface area between the ligand and protein that results from close and favorable contacts between atoms of opposite polarity. It thus resembles the short-range attractive

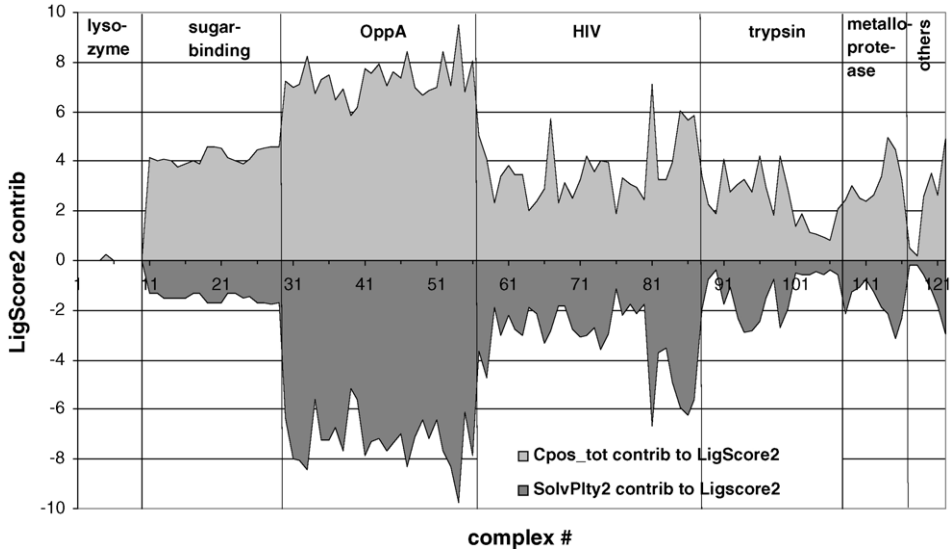

Fig. 8. Contributions to *LigScore2* of Cpos_tot and the SolvPlty^2 for 122 protein–ligand complexes with energy-minimized ligand poses. The numbering of the complexes is according to Table 1.

electrostatics of the protein–ligand complex, including hydrogen bonds that the ligand forms with polar or ionic functional groups of the protein.

The third and final descriptor used in the scoring functions, a desolvation penalty, turned out to be the most elusive one to identify. However, it is this term in particular that sets our scoring function apart from most other scoring functions that have been previously reported in the literature (see references above). For *LigScore1*, the desolvation penalty term is derived from the sum of squared attractive and repulsive protein–ligand contact terms. Accordingly, it decreases the score values in a way that mimics the quadratic charge dependency of the Born solvation energy of ions [45].

In the case of *LigScore2*, this idea further evolved into considering only the sum of squared terms that include the buried polar surface area of the ligand as well as the protein, respectively. In both cases, the contribution of desolvation tends to counterbalance favorable interactions established through polar contacts of the ligand binding to the protein receptor. This plays an important role in evaluating protein–ligand-binding affinities, and is underscored by the example of the OppA complexes. In addition to the OppA receptor sites consisting of a largely polar binding pocket, the tripeptide ligands of these systems contain two ionic lysine residues. Scoring functions that do not take into account the decrease in binding affinity resulting when waters solvating the tripeptide as well as the OppA receptor site are removed tend to overestimate the overall effects of favorable polar contacts that are formed upon binding. Since the *PLP* scoring function lacks such a desolvation term, it evidently overscores the OppA complexes (Fig. 7). Although other empirical affinity models, i.e. the *Jain* scoring function [22], have included solvation effects, the breakdown of individual contributions yielded only a marginal cost associated with desolvating a ligand or protein, i.e. 5% of *Jain* scores. In our analysis, we found that the desolvation term can significantly contribute to the overall *LigScore1* or *LigScore2* values. In the case of OppA complexes, the contributions of Cpos_tot and the desolvation penalty term effectively cancel each other out (Fig. 8).

One important finding of our scoring function analysis involves the fact that in order to optimize the correlation between predicted and experimental pK_i values, it was essential to first eliminate existing anomalies in the coordinates of the X-ray complexes by minimizing the protein–ligand interaction energies. These result in large van der Waals repulsions between ligand and protein atoms. Minimizing the ligand in the presence of the rigid protein relieved these steric clashes and let to better overall agreement with experiment. In future studies, we plan to extend this scheme in such a way as to optimize the training set with the scoring equation as the objective function. Utilizing an iterative optimization approach, first reported by Jain [22], of receptor–ligand configurations in combination with parameters of the scoring equation should further enhance the robustness of our scoring functions and their ultimate suitability for use as a combined docking and scoring function.

In summary, we report two new empirical scoring functions that possess high predictive accuracy of ligand–receptor-binding affinities over a wide range of protein classes as well as pK_i values, while consisting of only three physicochemical descriptors that can be readily related to fundamental molecular interactions.

Acknowledgements

We would like to thank Scott Kahn, Rod Hubbard, and Hugo Kubinyi for valuable discussions on this work. This research was supported in part by the Combinatorial Chemistry Consortium.

References

[1] B. Domon, S. Broder, Implications of new proteomics strategies for biology and medicine, J. Proteome Res. 3 (2004) 253–260.
[2] G. Chambers, L. Lawrie, P. Cash, G.I. Murray, Proteomics: a new approach to the study of disease, J. Pathol. 192 (2000) 280–288.
[3] L. Stein, Genome annotation: from sequence to biology, Nat. Rev. Genet. 2 (2001) 493–503.
[4] A.F. Yakunin, A.A. Yee, A. Savchenko, A.M. Edwards, C.H. Arrowsmith, Structural proteomics: a tool for genome annotation, Curr. Opin. Chem. Biol. 8 (2004) 42–48.
[5] E. Fischer, Einfluss der configuration auf die Wirkung der enzyme, Ber. Dtsch. Chem. Ges. 27 (1894) 85–93.
[6] D.E. Koshland, Application of a theory of enzyme specificity to protein synthesis, Proc. Natl. Acad. Sci. U.S.A. 44 (1958) 98–104.
[7] R. Wang, Y. Lu, S. Wang, Comparative evaluation of 11 scoring functions for molecular docking, J. Med. Chem. 46 (2003) 2287–2303.
[8] H. Gohlke, G. Klebe, Statistical potentials and scoring functions applied to protein–ligand binding, Curr. Opin. Struct. Biol. 11 (2001) 231–235.
[9] P.A. Kollman, Free energy calculations: applications to chemical and biochemical phenomena, Chem. Rev. 93 (1993) 2395–2417.
[10] J. Aqvist, V.B. Luzhkov, B.O. Brandsdal, Ligand binding affinities from MD simulations, Acc. Chem. Res. 35 (2002) 358–365.
[11] H.A. Carlson, W.L. Jorgensen, An extended linear response method for determining free energies of hydration, J. Phys. Chem. 99 (1995) 10667–10673.
[12] I. Muegge, Y.C. Martin, A general fast scoring function for protein–ligand interactions: a simplified potential approach, J. Med. Chem. 42 (1999) 791–804.
[13] J.B.O. Mitchell, R.A. Laskowski, A. Alex, J.M. Thornton, BLEEP-potential of mean force describing protein–ligand interactions. Part I. Generating potential, J. Comp. Chem. 20 (1999) 1165–1176.
[14] H. Gohlke, M. Hendlich, G. Klebe, Knowledge-based scoring function to predict protein–ligand interactions, J. Mol. Biol. 295 (2000) 337–356.
[15] A.V. Ishchenko, E.I. Shakhnovich, Small molecule growth 2001 (SMoG2001): an improved knowledge-based scoring function for protein–ligand interactions, J. Med. Chem. 45 (2002) 2770–2780.
[16] M. Feher, E. Deretey, S. Roy, BHB: a simple knowledge-based scoring function to improve the efficiency of database screening, J. Chem. Inf. Comput. Sci. 43 (2003) 1316–1327.
[17] G. Verkhivker, K. Appelt, S.T. Freer, J.E. Villafranca, Empirical free energy calculations of ligand–protein crystallographic complexes. Part I. Knowledge-based ligand–protein interaction potentials applied to

the prediction of human immunodeficiency virus 1 protease binding affinity, Protein Eng. 8 (1995) 677–691.
[18] A. Wallqvist, R.L. Jernigan, D.G. Covell, A preference-based free-energy parameterization of enzyme-inhibitor binding. Applications to HIV-1-protease inhibitor design, Protein Sci. 4 (1995) 1881–1903.
[19] H.J. Böhm, Prediction of binding constants of protein ligands: a fast method for the prioritization of hits obtained from de novo design or 3D database search programs, J. Comput. Aided Mol. Des. 12 (1998) 309–323.
[20] D.K. Gehlhaar, G.M. Verkhivker, P.A. Rejto, C.J. Sherman, D.B. Fogel, L.J. Fogel, S.T. Freer, Molecular recognition of the inhibitor AG-1343 by HIV-1 protease: conformationally flexible docking by evolutionary programming, Chem. Biol. 2 (1995) 317–324.
[21] G.M. Verkhivker, D. Bouzida, D.K. Gehlhaar, P.A. Rejto, S. Arthurs, A.B. Colson, S.T. Freer, V. Larson, B.A. Luty, T. Marrone, P.W. Rose, Deciphering common failures in molecular docking of ligand–protein complexes, J. Comput. Aided Mol. Des. 14 (2000) 731–751.
[22] A.N. Jain, Scoring noncovalent protein–ligand interactions: a continuous differentiable function tuned to compute binding affinities, J. Comput. Aided Mol. Des. 10 (1996) 427–440.
[23] R.D. Head, M.L. Smythe, T.I. Oprea, C.L. Waller, S.M. Green, G.R. Marshall, VALIDATE: a new method for the receptor-based prediction of binding affinities of novel ligands, J. Am. Chem. Soc. 118 (1996) 3959–3969.
[24] M. Rarey, B. Kramer, T. Lengauer, G. Klebe, A fast flexible docking method using an incremental construction algorithm, J. Mol. Biol. 261 (1996) 470–489.
[25] M.D. Eldridge, C.W. Murray, T.R. Auton, G.V. Paolini, R.P. Mee, Empirical scoring functions. Part I. The development of a fast empirical scoring function to estimate the binding affinity of ligands in receptor complexes, J. Comput. Aided Mol. Des. 11 (1997) 425–445.
[26] R. Wang, L. Lai, S. Wang, Further development and validation of empirical scoring functions for structure-based binding affinity prediction, J. Comput. Aided Mol. Des. 16 (2002) 11–26.
[27] A.E. Muryshev, D.N. Tarasov, A.V. Butygin, O.Y. Butygina, A.B. Aleksandrov, S.M. Nikitin, A novel scoring function for molecular docking, J. Comput. Aided Mol. Des. 17 (2003) 597–605.
[28] T.I. Oprea, G.R. Marshall, Receptor-based prediction of binding activities, in: H. Kubinyi, G. Folkers, Y.C. Martin (Eds.), 3D QSAR in Drug Design: Ligand–Protein Interactions and Molecular Similarity, vol. 2, Kluwer Academic Publisher/Escom, Dortrecht, 1998, pp. 35–61.
[29] T.G. Davies, R.E. Hubbard, J.R. Tame, Relating structure to thermodynamics: the crystal structures and binding affinity of eight OppA-peptide complexes, Protein Sci. 8 (1999) 1432–1444.
[30] S.H. Sleigh, P.R. Seavers, A.J. Wilkinson, J.E. Ladbury, J.R. Tame, Crystallographic calorimetric analysis of peptide binding to OppA protein, J. Mol. Biol. 291 (1999) 393–415.
[31] Insight II, Version 2000.2, Accelrys Inc., San Diego, CA, 2002.
[32] Cerius2, Version 4.8, Accelrys Inc., San Diego, CA, 2002.
[33] U. Dinur, A.T. Hagler, New approaches to empirical force fields, in: K.B. Lipkowitz, D.B. Boyd (Eds.), Reviews in Computational Chemistry, vol. 2, VCH Publishers, New York, 1991, pp. 99–164.
[34] J.R. Maple, U. Dinur, A.T. Hagler, Derivation of force fields for molecular mechanics and dynamics from ab initio energy surfaces, Proc. Natl. Acad. Sci. USA 85 (1988) 5350–5354.
[35] Z. Peng, C.S. Ewig, M.-J. Hwang, M. Waldman, A.T. Hagler, Derivation of class II force fields. Part 4. van der Waals parameters of alkali metal cations and halide anions, J. Phys. Chem. A 101 (1997) 7243–7252.
[36] T.J. Ewing, S. Makino, A.G. Skillman, I.D. Kuntz, Dock 4. 0: search strategies for automated molecular docking of flexible molecule databases, J. Comput. Aided Mol. Des. 15 (2001) 411–428.
[37] S.L. Mayo, B.D. Olafson, W.A.I. Goddard, DREIDING: a generic force field for molecular simulations, J. Phys. Chem. 94 (1990) 8897–8909.
[38] J. Gasteiger, M. Marsili, A new model for calculating atomic charges in molecules, Tetrahedron Lett. (1978) 3181–3184.
[39] C.M. Venkatachalam, X. Jiang, T. Oldfield, M. Waldman, LigandFit: a novel method for the shape-directed rapid docking of ligands to protein active sites, J. Mol. Graphics Modell. 21 (2003) 289–307.
[40] M. Levitt, Protein folding by restrained energy minimization and molecular dynamics, J. Mol. Biol. 170 (1983) 723–764.
[41] D. Rogers, A.J. Hopfinger, Application of genetic function approximation to quantitative structure–activity relationships and quantitative structure property relationships, J. Chem. Inf. Comput. Sci. 34 (1994) 854–866.
[42] D. Rogers, Evolutionary statistics: using a genetic algorithm and model reduction to isolate alternate statistical hypothses of experimental data, in: Proceedings of the Seventh International Conference on Genetic Algorithm, East Lansing, MI, 1997.
[43] H.J. Böhm, The development of a simple empirical scoring function to estimate the binding constant for a protein–ligand complex of known three-dimensional structure, J. Comput. Aided Mol. Des. 8 (1994) 243–256.
[44] L.T. Chong, S.E. Dempster, Z.S. Hendsch, L.P. Lee, B. Tidor, Computation of electrostatic complements to proteins: a case of charge stabilized binding, Protein Sci. 7 (1998) 206–210.
[45] M. Born, Volumen und Hydratationswärme der Ionen, Z. Phys. 1 (1920) 45–48.
[46] N.M. Green, Avidin, Adv. Protein Chem. 29 (1975) 85–133.